Hindawi
Journal of Chemistry
Volume 2017, Article ID 7590506, 13 pages
https://doi.org/10.1155/2017/7590506

Research Article

Equilibrium Measurements of the NH_3-CO_2-H_2O System: Speciation Based on Raman Spectroscopy and Multivariate Modeling

Maths Halstensen,[1] Henrik Jilvero,[2] Wathsala N. Jinadasa,[1] and Klaus-J. Jens[1]

[1]*Applied Chemometrics Research Group (ACRG), University College of Southeast Norway, Porsgrunn, Norway*
[2]*Department of Energy and Environment, Chalmers University of Technology, 412 96 Göteborg, Sweden*

Correspondence should be addressed to Maths Halstensen; maths.halstensen@usn.no

Received 29 December 2016; Revised 14 March 2017; Accepted 4 April 2017; Published 11 May 2017

Academic Editor: Adriano A. Gomes

Liquid speciation is important for reliable process design and optimization of gas-liquid absorption process. Liquid-phase speciation methods are currently available, although they involve tedious and time-consuming laboratory work. Raman spectroscopy is well suited for in situ monitoring of aqueous chemical reactions. Here, we report on the development of a method for speciation of the CO_2-NH_3-H_2O equilibrium using Raman spectroscopy and PLS-R modeling. The quantification methodology presented here offers a novel approach to provide rapid and reliable predictions of the carbon distribution of the CO_2-NH_3-H_2O system, which may be used for process control and optimization. Validation of the reported speciation method which is based on independent, known, NH_3-CO_2-H_2O solutions shows estimated prediction uncertainties for carbonate, bicarbonate, and carbamate of 6.45 mmol/kg H_2O, 34.39 mmol/kg H_2O, and 100.9 mmol/kg H_2O, respectively.

1. Introduction

The rapid increase in the level of CO_2 in the earth's atmosphere is recognized as the single most important environmental challenge facing our global society [1]. All climate change mitigation plans rely on carbon dioxide capture and storage as a near-term "immediate response" technology [2]. Despite the various global CO_2 capture research and development initiatives, the well-established gas-liquid absorption process is expected to be the technology of choice for early, large-scale deployment [3], with the chilled ammonia process (CAP) [4] being one of the currently demonstrated technologies.

Out of several postcombustion techniques available to capture CO_2 from coal power plants, amine solutions have been commonly tested and used. The disadvantages of amine technology are that it requires large amount of energy in the stripping process and has thermal and oxidative degradation and corrosion problems [5]. Ammonia technology is an alternative to overcome these drawbacks. This process requires less energy for stripping and the heat of reaction is much lower than amine process. There is less maintenance cost than amine process as there are no degradation or corrosion issues. CO_2 reacted ammonia can be used to produce fertilizer. The process of CO_2 capture by ammonia can be twofold depending on the temperature of CO_2 absorption. If the absorption is performed under 2–10°C, which is called the chilled ammonia process, there can be precipitations of ammonium carbonate compounds while if the absorption is increased to 25–40°C, the precipitation problem is eliminated [6].

If chemical speciation data could be generated concomitant with the determination of the physical and chemical solvent properties, the development and accuracy of the thermodynamic process model would be greatly facilitated. Improvement and optimization of commercial processes that target needed cost reductions require access to rigorous thermodynamic models that build on liquid-phase speciation data. Such data are currently acquired through tedious and time-consuming laboratory work. The standard

wet chemistry titration to determine liquid phase is the most popular method. This method takes time and errors can be propagated during sampling, chemical preparation, weighing, and titration [7]. Various analytical techniques can be used to determine the species present in CO_2 reacted ammonia solution. ^{13}C nuclear magnetic resonance (NMR) spectroscopy has been used [8] to determine ionic species in a range of ammonia concentration from 0.69 to 8.95 mol/L and CO_2 loading (total CO_2 moles/initial solvent moles) concentrations from 0.33 to 0.72. Fourier transform infrared spectroscopy (FT-IR) and X-ray diffraction (XRD) were used to qualitatively distinguish ammonium bicarbonate from ammonium carbonate and ammonium carbamate, while CHN elemental analysis and near-infrared (NIR) spectroscopy were used to quantify ammonium bicarbonate based on multivariate regression methods as reported in [9]. Wen and Brooker [10], Zhao et al. [11], and Kim et al. [12] suggested methods to determine carbon species in CO_2-NH_3-H_2O system based on factor analysis where they assumed that the corresponding Raman intensities were directly related to the concentrations of species.

This work reports on a method that combines Raman spectroscopy and partial least-squares regression (PLS-R) for in situ solvent speciation in the chilled ammonia process and which does not rely on calibration by an independent analysis method [13], for example, NMR. It describes the development, validation, and application of the method for determination of the liquid phase composition of the NH_3-CO_2-H_2O system, while comparisons of the speciation results obtained here and those from established CO_2-NH_3-H_2O thermodynamic equilibrium models are described in a separate publication [14].

In the thermodynamic modeling of the CO_2-NH_3-H_2O system, a vapor-liquid equilibrium (VLE) is assumed to exist for water, ammonia, and CO_2. The liquid phase can be described by reactions (1)–(5). The chemical composition of aqueous ammonia solution is described by

$$NH_3 + H_2O \rightleftarrows NH_4^+ + OH^- \quad (1)$$

The reactions of dissolved CO_2 in aqueous ammonia solution are given by reactions (2)–(5). Within the present system, CO_2 is bound as the anion species of carbonate $[CO_3^{2-}]$, bicarbonate $[HCO_3^-]$, and carbamate $[NH_2COO^-]$.

$$CO_{2(aq)} + H_2O \rightleftarrows H^+ + HCO_3^- \quad (2)$$

$$HCO_3^- \rightleftarrows H^+ + CO_3^{2-} \quad (3)$$

$$CO_{2(aq)} + 2NH_3 \rightleftarrows NH_4^+ + NH_2COO^- \quad (4)$$

$$NH_4^+ + NH_2COO^- + H_2O \rightleftarrows NH_4^+ + HCO_3^- + NH_3 \quad (5)$$

During CO_2 absorption by the aqueous NH_3 solution, reactions (1)–(5) will equilibrate according to the CO_2 concentration, pressure, and temperature; the carbon distribution in the solvent is given by the concentrations of the anions in reactions (2)–(5). In addition to these reactions and depending on the reaction conditions, various other compounds may precipitate, such as ammonium bicarbonate (NH_4HCO_3), ammonium carbonate $[(NH_4)_2CO_3]$, ammonium carbamate ($NH_4NH_2CO_2$), and ammonium sesquicarbonate $[(NH4)_2CO_3{\cdot}NH_4HCO_3]$. Even though the precipitation is promoted by low temperature, the high water content in the solvent reduces much of this possibility.

Spectroscopy, Raman spectroscopy in particular, is well known for in situ monitoring of the chemical reactions of aqueous solutions [16, 17]. The water molecule shows only weak Raman scattering; hence Raman spectroscopy has potential advantage over IR spectroscopy [18] for aqueous phase analysis such as required for the aqueous chilled ammonia CO_2 capture solvent. The Raman band envelopes of aqueous solutions of ammonium carbonate, ammonium bicarbonate, and ammonium carbamate have been identified and analyzed [10] and form the basis for the previously reported speciation studies of the CO_2-NH_3-H_2O system [11, 12]. However, evaluation of the Raman spectra in these previous studies was based on univariate, single-band analysis. The use of superior multivariate partial least-squares regression (PLS-R) [19] methods, which exploit the multivariate information in the spectra, has, to the best of our knowledge, not been reported previously. Furthermore, the method developed in the present study is not limited to laboratory applications but can also be used to monitor continuously a reactive process, which presents an opportunity for its implementation as an on-line process analytical technology (PAT) [20] in carbon capture plants for optimization and efficient operation.

2. Materials and Methods

The development of the Raman spectroscopy-based method for speciation of the CO_2-NH_3-H_2O system is based on PLS-R analysis of a series of samples of known composition. The procedure involves

(1) preparation of aqueous solutions that contain known concentrations of $[CO_3^{2-}]$, $[HCO_3^-]$, and $[NH_2COO^-]$: one set of solutions was prepared for PLS-R model calibration and a second independent set of solutions was used for validation;

(2) determination of the Raman spectrum of each sample solution;

(3) preprocessing of the Raman spectra by cropping each spectrum to cover the range 450–2300 cm^{-1}, with subsequent elimination of the inconsistently varying baseline from spectrum-to-spectrum and centering of each wavelength by subtraction of the mean;

(4) calibration of the PLS-R models for the anionic species $[CO_3^{2-}]$, $[HCO_3^-]$, and $[NH_2COO^-]$ using the Raman spectra of the solutions prepared for model calibration in the previous step (Step (3));

(5) validation of the PLS-R models using the Raman spectra of the solutions prepared for model validation in Step (3).

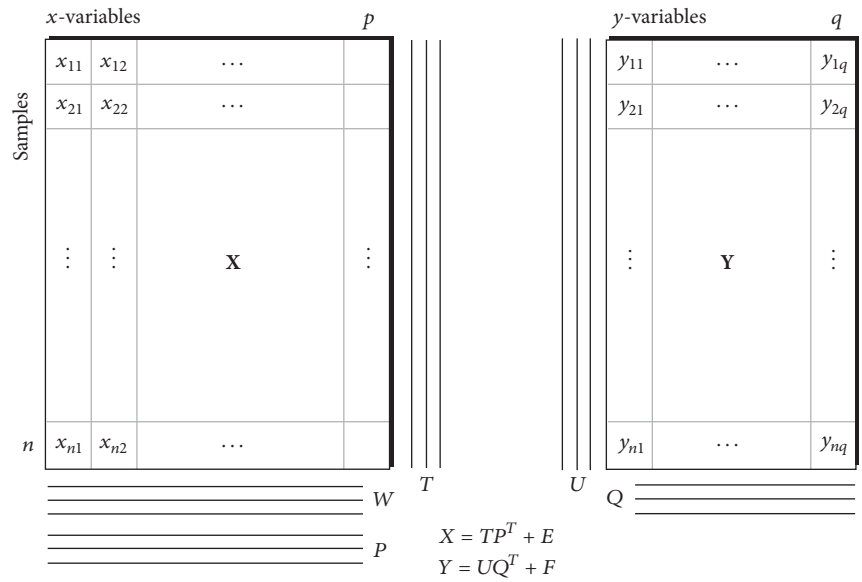

Figure 1: X-Y data and models in the PLS-R modeling approach [15]. The parameters that emanate from PLS-R calibration include P (X loadings); W (X loading weights); T (X scores); U (Y scores); and Q (Y loadings). E and F are the residuals for X and Y, respectively.

The procedures required to achieve reliable speciation using the proposed method are described in the following sections.

2.1. Raman Spectroscopy. The Raman phenomenon is based on quantized vibrational changes that are associated with electromagnetic radiation absorption. An important advantage of Raman spectroscopy over infrared spectroscopy is that the water molecule shows very weak Raman scattering, whereas, in infrared spectroscopy, the water molecule shows strong absorption across an important part of the infrared spectrum.

The Raman instrument used in the investigations reported in the present paper was the RXN2 portable multichannel Raman spectrometer (Kaiser Optical Systems Inc.). Four fiber optic probes can be connected and utilized through an automatic sequential scanning system that is integrated into the instrument. The specifications of the RXN2 Raman spectrometer are listed in Table 1.

Raman spectra of aqueous solutions can be acquired using either a noncontact probe optic, whereby the sample solutions are not in direct contact with the probe optic, or an immersion probe optic, whereby the sample solution is in direct contact with the probe optic. The Raman spectra were acquired using a short-focus (200 μm), sapphire window, Hastelloy immersion probe (Kaiser Optical Systems Inc.).

Table 1: Specifications of the RXN2 Raman spectrometer.

Name	Description
Excitation laser wavelength (nm)	785
Spectral range (cm^{-1})	100–3425
Spectral resolution (cm^{-1})	4
Operating temperature range (°C)	15–30
Number of channels	4
Laser type	Invictus™ NIR diode laser
Spectrograph	f/1.8 Holographic imaging spectrograph
Grating	Holographic transmission grating
Detector	TE cooled, 1024 CCD Detector
Multichannel scanning	4-Channel sequential operation
Cal-Check™	Automatic analyzer monitor
Auto-Cal™	Automated calibration of axis and laser wavelength
Immersion probe optic	200 μm (short focus)/Hastelloy/sapphire window

2.2. Partial Least-Squares Regression Modeling. PLS-R is an empirical data-driven modeling approach that requires both representative input data (X) and output data (Y). A detailed description of PLS-R and validation can be found in literature [15, 19, 21]. In this study PLS-R is used in combination with Raman spectroscopy. The X matrix contains Raman spectra that represent different concentrations and the Y vector contains known reference concentrations from the sample preparation step. All models reported in this article are validated based on independent test data (test set validation) [21].

The concentration range spanned by X and Y should reflect the concentrations to be predicted. The overall aim of PLS-R is to model simultaneously the multivariate input data (X) and the output response (Y) (Figure 1). PLS-R avoids many of the problems associated with the traditional multiple

linear regression (MLR) and principal component regression (PCR) [15] methods. PLS-R is advantageous in cases where the X matrix contains collinear data. Colinearity is in most cases unavoidable in spectroscopy, as there are significantly more variables (waveshifts) than samples (observations). When the number of variables is significantly higher than the number of samples, colinearity is guaranteed. When collinear data are used, MLR fails or becomes unstable. Although PCR can deal with colinearity, it has other issues related to the way in which the X-matrix is decomposed without utilizing information on Y, often leading to models with a higher number of components than the PLS-R case. Another advantage of applying PLS-R is that the feature parameters that emerge from the model calibration stage, that is, X scores (T), X loadings (P), X loading weights (W), and Y scores (U), can be plotted and interpreted to support the calibration procedure (see Figure 1).

An important aspect of PLS-R modeling is model validation [21], which is important to determine the complexity of the model. The correct complexity of a PLS-R model is defined as the optimal number of PLS components, which can only be determined by proper validation of the model using an independent dataset that is acquired and used exclusively for this purpose. To determine the optimal number of components in a PLS-R model, a criterion based on the so-called root mean square error of prediction (RMSEP) [15] is calculated and minimized. RMSEP is based on predictions of Y, for example, concentrations from the validation dataset. Using several models with different numbers of components, the predictions are compared to the reference values of Y in the RMSEP calculation. The model that has the optimal number of components is defined as the one that ends up with the lowest RMSEP value. The RMSEP values are derived using (6):

$$\text{RMSEP} = \sqrt{\frac{\sum_{i=1}^{I} \left(\mathbf{y}_{\text{predicted}} - \mathbf{y}_{\text{reference}}\right)^2}{I}}, \tag{6}$$

where $\mathbf{y}_{\text{predicted}}$ is the predicted value from the PLS-R model, which is compared to the reference value $\mathbf{y}_{\text{reference}}$. The sum of the squared prediction errors is divided by I, which is the number of samples in the validation dataset.

2.3. Preparation of the Calibration and Validation Samples. The ranges of concentrations, expressed in moles of each anion per kilogram of H_2O (molality), of the calibration and validation set were predetermined to reflect the concentrations expected in samples that would in the future be subjected to the developed speciation method. The calibration and validation sets covered the same concentration range. Analytical grade chemicals and Milli-Q water (18.2 MΩ·cm) were used to prepare the samples. The ammonia solution (25 wt%) was supplied by Merck KGaA (Darmstadt, Germany). Sodium hydrogen bicarbonate (99.7%), sodium carbonate (99.9%), and ammonium carbamate (98%) were supplied by Sigma-Aldrich (Steinheim, Germany). All chemicals were used as received. All solutions were prepared gravimetrically using a Mettler Toledo balance (±0.1 mg). Forty solutions of each of Na_2CO_3, $NaHCO_3$, and $NH_4NH_2CO_2$, spanning the concentration ranges of 0–0.7 mol/kg H_2O, 0–0.96 mol/kg H_2O, and 0–2.56 mol/kg H_2O, respectively, were prepared for calibration and validation purposes.

The selection of concentration range for calibration and validation range is important especially when the model is used for analyzing future samples. Three factors were considered during this selection which are the solubility of the chemicals, expected species concentrations, and Raman instrument performance. As reported in [22], solubility of Na_2CO_3 is 0.7 g at 0°C and 1.25 g at 10°C per kg H_2O. $NaHCO_3$ solubility in water is 0.69 g at 0°C and 0.815 g at 10°C per kg H_2O. Ammonium carbamate is freely soluble in water. Holmes et al. [8] report a comparison of equilibrium measurements of ionic system in CO_2-NH_3-H_2O systems for different initial concentrations of CO_2 loading. The comparison is based on his experimental work on ^{13}C NMR measurements with three thermodynamic models of Pitzer model [23], NRTL model [24], and TIDES model [25]. This comparison gives an indication of expected species concentration for a given CO_2 loading and NH_3 concentration. For the demonstration of the proposed method in this study, different samples prepared using 5 wt% ammonia in the CO_2 loading range from 0 to 0.6 mol CO_2/mol NH_3 were used and the expected species concentration reasonably falls in the calibration and validation range based on the reported work by Holmes et al. [8]. The limitation of the Raman instrument was also considered when selecting the concentration range. An overview of the sample solutions used for the calibration and validation of the PLS-R models, including the respective concentrations, can be found in Appendix.

2.4. Acquisition of Raman Spectra. The Raman spectra were measured with the Kaiser RXN2 Raman spectrometer using a laser power of 400 mW and a total exposure time of 60 seconds with six scans of 10 seconds each being applied to achieve a good signal-to-noise ratio. To maintain a consistent temperature in the spectrometer, the instrument was stabilized for 30 minutes before each measurement series. The short-focus immersion optic was fitted onto the fiber optic probe head and cleaned with acetone. The immersion probe was then positioned vertically using a stand, with the optical window facing down. A glass container that contained the sample solution was positioned under the immersion optic, which was then carefully immersed in the solution. The tip of the optic was positioned in the center of the solution, approximately 20 mm from the bottom of the glass container. The sample and probe optic were protected from external light sources (such as fluorescent light) using aluminum foil. The Raman spectrum was obtained by initiating a scan in the instrument software. In the intervals between sample measurements, the probe was cleaned in acetone to avoid cross-contamination of sample solutions.

2.5. Preprocessing of Raman Spectra. Figure 2 presents an example of the preprocessing of the Raman spectra (calibration and validation samples for bicarbonate). During preprocessing, all the Raman spectra were cropped so as to cover the range of 450–2300 cm^{-1}, since wavelengths outside

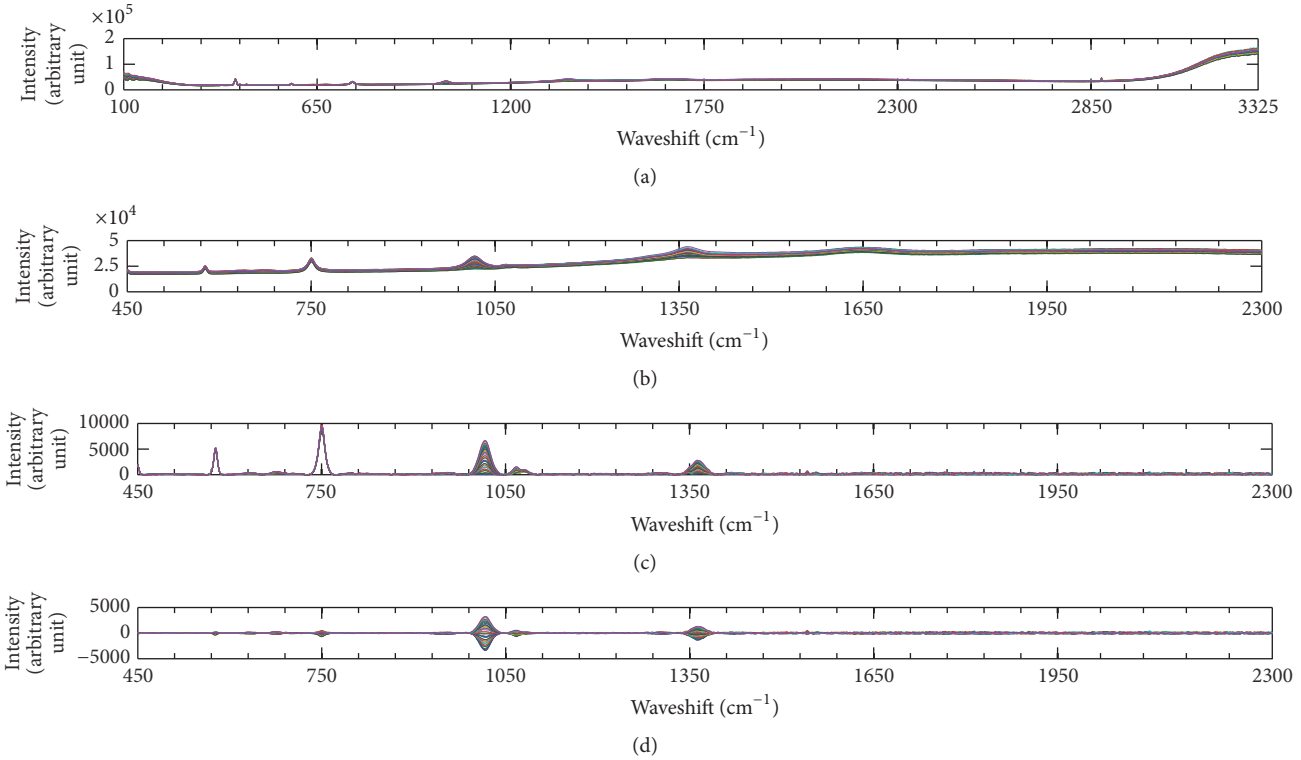

Figure 2: Preprocessing steps of the calibration and validation Raman spectra of bicarbonate. (a) Raw spectra for the range of 100–3325 cm^{-1}. (b) Spectra cropped to cover the range of 450–2300 cm^{-1}. (c) Spectra baseline corrected using the Whittaker filter (lambda = 100; $P = 0.001$). (d) Mean-centered spectra for PLS-R model calibration.

this range were not useful for the PLS-R analysis. Figures 2(a) and 2(b) show the bicarbonate spectra before and after cropping, respectively. In this range, the Raman spectra show an inconsistent baseline, which is particularly evident at the highest Raman shifts (above 2000 cm^{-1}). Raman spectra with variable baselines often generate regression models that have a higher number of components than is necessary, since the model also needs to model the baseline drift. To ensure a less complex model, a baseline correction is performed to decrease or remove the baseline drift in each Raman spectrum. Several baseline correction methods are available [26]. Spectroscopic data from a Raman spectrometer can be decomposed into three parts: (1) the analytical signal; (2) the baseline; and (3) noise. Noise was not a problem in the present study, whereas the baseline required some attention. The goal of all the baseline correction methods is to estimate the baseline in order to remove it. The MATLAB® 2012b software (MathWorks Inc.) in combination with PLS Toolbox 7.31 (Eigenvector Research Inc.) was used to find a suitable baseline correction in the present case. The lowest RMSEP was gained using the Whittaker filtering method [27] included in PLS Toolbox 7.31, which preserves the original shape of the signal part of the Raman spectrum. The Whittaker filter was applied with the following parameters: lambda = 100 and $P = 0.001$. The lambda parameter defines how much curvature is allowed, while the P parameter holds information about asymmetry in the spectra. Figure 2(c) shows the Raman spectra of bicarbonate after baseline correction using the Whittaker filter. Finally, the spectra were centered by subtracting the mean from each variable (waveshift) in the Raman spectra. Centering [19] is applied prior to PLS-R calibration to avoid the need for an additional PLS-component to describe the mean of the data, which would entail a more complex model. Figure 2(d) shows the data after mean-centering. To summarize, the spectra were cropped to lie within the range of 450–2300 cm^{-1}, the baseline was corrected using the Whittaker filter with lambda value of 100 and P value of 0.001, and the spectra were centered on the mean prior to calibration of the PLS-R models of the three species (carbonate, bicarbonate, and carbamate).

2.6. PLS-R Modeling of Carbonate, Bicarbonate, and Carbamate. Individual models for carbonate, bicarbonate, and carbamate were calibrated based on the obtained Raman spectra of aqueous solutions that contained known concentrations in the ranges of 0–0.7 mol/kg, 0–0.96 mol/kg, and 0–2.56 mol/kg, respectively. Since the aim was to develop PLS-R models that could be used for speciation of a real CO_2-NH_3-H_2O system, a selection of variables (waveshifts) to be included in each model was carried out. The waveshifts to be included in the model of each respective anion were chosen based on backward selection, whereby only the wavelengths related to ammonia and the other two CO_2 anion species were omitted. In the model for the prediction of carbonate, the Raman wavelengths associated with ammonia,

Table 2: Vibrational assignments of $(NH_4)_2CO_3$, NH_4HCO_3, and $H_2NCOONH_4$ aqueous solutions, and omitted frequencies in the respective PLS-R models. Adapted from the data of Wen and Brooker [10].

Frequency [cm^{-1}]	Assignment	Omitted frequencies for the PLS-R anion model		
		Carbonate	Bicarbonate	Carbamate
3390	Antisymmetric N-H stretch of NH_3	X	X	X
3310	Symmetric N-H stretch of NH_3	X	X	X
3220	Fermi resonance with N-H symmetry stretch of NH_3	X	X	X
3050	Symmetric N-H stretch of NH_4^+	X	X	X
2850	A combination of fundamentals of NH_4^+	X	X	X
1690	NH_2 deformation of NH_4^+	X	X	X
1645	Antisymmetric deformation of NH_3			X
1630	C-O antisymmetric stretch of HCO_3^-			X
1550	Antisymmetric CO_2 stretch of H_2NCOO^-			X
1436, 1380	CO antisymmetric stretch of CO_3^{2-}	X, X	X, X	X, X
1430	Antisymmetric NH_2 deformation of NH_4^+	X	X	X
1405	Symmetric CO_2 stretch of H_2NCOO^-	X	X	X
1360	CO symmetric stretch of HCO_3^-	X		X
1302	C-OH bend of HCO_3^-	X	X	X
1120	CN stretch of H_2NCOO^-	X	X	X
1065	CO symmetric stretch of CO_3^{2-}		X	X
1034	NH_2 wag of H_2NCOO^-	X	X	
1017	C-OH stretch of HCO_3^-	X	X	X
680	CO_2 antisymmetric deformation of CO_3^{2-}	X	X	X
640	(OH)-CO bend of HCO_3^-	X	X	X
570	Torsion about CO_2 skeleton of H_2NCOO^-	X	X	X

bicarbonate, and carbamate were omitted. The wavelength ranges used in the modeling of bicarbonate analysis were selected based on the same principle, while the carbamate model was based on a more limited range of wavelengths. Since PLS-R modeling of carbamate is more challenging than modeling of the other two species, forward selection was used to define the wavelength ranges in this model. Fine-tuning of the wavelength selection was made based on prediction results, in which the model with a combination of variables that resulted in the lowest prediction uncertainty was used. The carbonate, bicarbonate, and carbamate models were based on the respective frequency ranges of [450–520, 750–950, 1062–1100, 1140–1200, 1520–1650 and 1760–2300] cm^{-1}; [450–520, 750–950, 1140–1200, 1350–1390, 1520–1650 and 1760–2300] cm^{-1}; and [1033–1043] cm^{-1}. Table 2 lists the frequencies omitted from each PLS-R anion model.

The PLS-R models for carbonate, bicarbonate, and carbamate were all based on 20 calibration spectra, in addition to the 20 independent spectra that were used exclusively for the validation. Figure 3 shows the spectra used to calibrate and validate the carbonate, bicarbonate, and carbamate prediction models.

Dissolution of carbonate in water will lead to the following equilibrium state as given in reaction (7).

$$CO_3^{2-} + H_2O \rightleftarrows OH^- + HCO_3^- \quad (7)$$

However, given the detection limit of the Raman spectrometer, only the carbonate band was observed. Therefore, this reaction was neglected in the carbonate PLS-R model development. However, in the cases of bicarbonate dissolution, reaction (8) and for carbamate dissolution reactions (7)–(13) were observed.

$$HCO_3^- \rightleftarrows H^+ + CO_3^{2-} \quad (8)$$

$$CO_3^{2-}{}_{(aq)} + NH_4^+{}_{(aq)} \rightleftarrows HCO_3^-{}_{(aq)} + NH_{3(aq)} \quad (9)$$

$$NH_3 + H_2O \rightleftarrows NH_4^+ + OH^- \quad (10)$$

$$NH_4^+ \rightleftarrows H^+ + NH_3 \quad (11)$$

$$HCO_3^-{}_{(aq)} + NH_{3(aq)} \rightleftarrows H_2NCOO^-{}_{(aq)} + H_2O \quad (12)$$

$$H_2NCOO^-{}_{(aq)} + H_2O \rightleftarrows CO_3^{2-}{}_{(aq)} + NH_4^+{}_{(aq)} \quad (13)$$

Thus, the quantitative PLS-R models were developed according to the following steps:

(1) Calibrate and validate the carbonate model.

(2) Predict carbonate in the bicarbonate calibration and validation datasets, and correct the bicarbonate references accordingly.

(3) Calibrate and validate the bicarbonate model based on the corrected dataset obtained in Step (2).

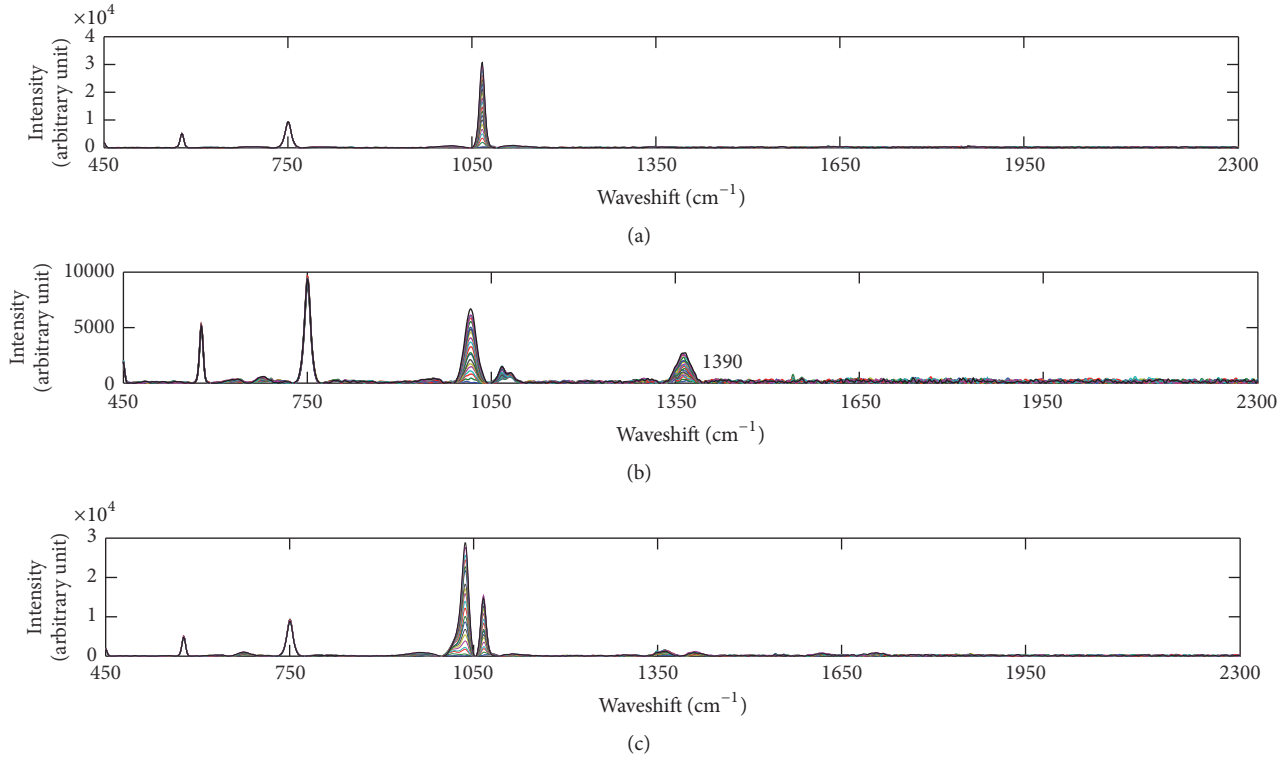

Figure 3: Raman spectra used in the PLS-R model calibration and validation. (a) Raman spectra of carbonate; (b) Raman spectra of bicarbonate; (c) Raman spectra of carbamate.

(4) Apply the carbonate model from Step (1) and bicarbonate model from Step (3) to predict carbonate and bicarbonate in the carbamate calibration and validation datasets.

(5) Correct the carbamate references in the calibration and validation datasets based on the predictions of carbonate and bicarbonate made in Step (4).

(6) Calibrate and validate the carbamate model.

All the PLS-R models developed in the present study were developed using the Unscrambler X ver. 10.3 software. Finally, the speciation method was demonstrated based on realistic aqueous solutions that contained 5 wt% ammonia loaded with CO_2. Since reference concentrations for carbonate, bicarbonate, and carbamate are not available for these datasets, the prediction results were assessed based on the calculated prediction uncertainties provided by Unscrambler X ver. 10.3.

3. Results and Discussion

The calibration and validation results for each of the respective PLS-R models for carbonate, bicarbonate, and carbamate are presented in the respective subsections below. Outliers were detected in the validation and calibration sets for carbonate using the $t_1 - u_1$ scatter plots (data not shown). An outlier may result from an air bubble sticking to the sapphire window in the tip of the probe optic or from the probe optic being inserted so far down into the solution that the measurement is influenced by the glass container.

3.1. PLS-R Validation Results for Carbonate, Bicarbonate, and Carbamate. Figures 4–6 show the validation results for the PLS-R models of carbonate, bicarbonate, and carbamate, respectively. The results include plots of the scores ($t_1 - t_2$), regression coefficients (B), residual validation variances, and predicted concentrations versus the reference concentrations. The score plots are used to visualize how the calibration spectra compare to the validation spectra. The regression coefficients show the weight that each wavelength is assigned in the prediction. The residual validation variance plot shows the size of the residual for models with an increasing number of components. The predicted versus measured plots show how the predicted concentrations from the validation dataset in comparison with the references calculated from the sample preparation stage. Prediction performance is evaluated from an interpretation of the statistical parameters of merit, which include r^2, RMSEP, and the slope of the regression line.

For the carbonate series, one outlier, identified according to the definition provided previously [19], was removed from the validation dataset. No outliers were detected in the calibration dataset. The outlier was not considered thereafter. Figure 4 shows selected plots from the calibration and validation of the PLS-R model for carbonate. In bicarbonate series no outliers were detected in the calibration and validation datasets. Figure 5 shows selected plots from the calibration

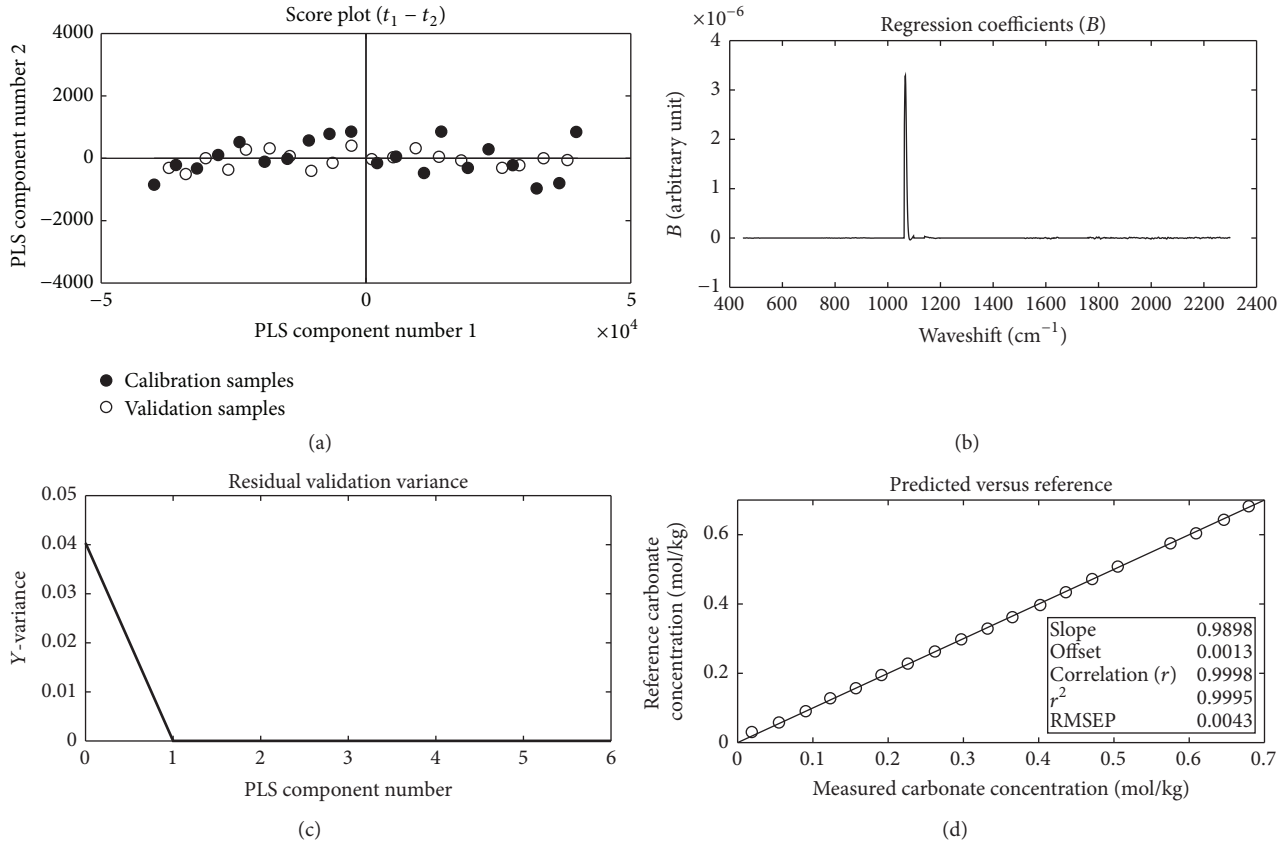

Figure 4: PLS-R model for carbonate. (a) Score plot of PLS components 1 versus 2 showing the calibration samples and validation samples. (b) Regression coefficients based on a one-component PLS-R model. (c) The residual validation variance shows that one PLS-component is optimal. (d) Predicted carbonate concentrations based on the one-component PLS-R model versus the reference concentrations obtained from the solute ion preparation stage.

Table 3: PLS-R modeling of carbonate, bicarbonate, and carbamate.

Model	Carbonate model	Bicarbonate model	Carbamate model
Wavelength ranges included [cm^{-1}]	450–520, 750–950, 1062–1100, 1140–1200, 1520–1650 and 1760–2300	450–520, 750–950, 1140–1200, 1350–1390, 1520–1650 and 1760–2300	1033–1043
Slope	0.9898	0.9636	1.0246
r^2	0.9995	0.9932	0.9968
RMSEP [mmol/kg]	4.3	24.1	49.9
Number of components	1	1	1
Number of outliers	1 (in the validation set)	0	0

and validation of the PLS-R model for bicarbonate. For carbamate series also no outliers were detected in the calibration or validation datasets. Figure 6 shows selected plots from the calibration and validation of the PLS-R model for carbamate.

The wavelength ranges used in the PLS-R models for the predictions of carbonate, bicarbonate, and carbamate are presented in Table 3. Some variables (waveshifts) with regression coefficients close to zero were also included, as it was found that the prediction uncertainties were slightly improved when these wavelengths were included. The values for the slope, r^2, RMSEP, the number of PLS components, and outliers in all three models are listed in Table 3.

Multivariate analysis has been proven to overcome many challenges in univariate method. Univariate method is simple and samples for calibration can be prepared using one chemical when there are no interferences from other constituents. There are many instances when the property of interest

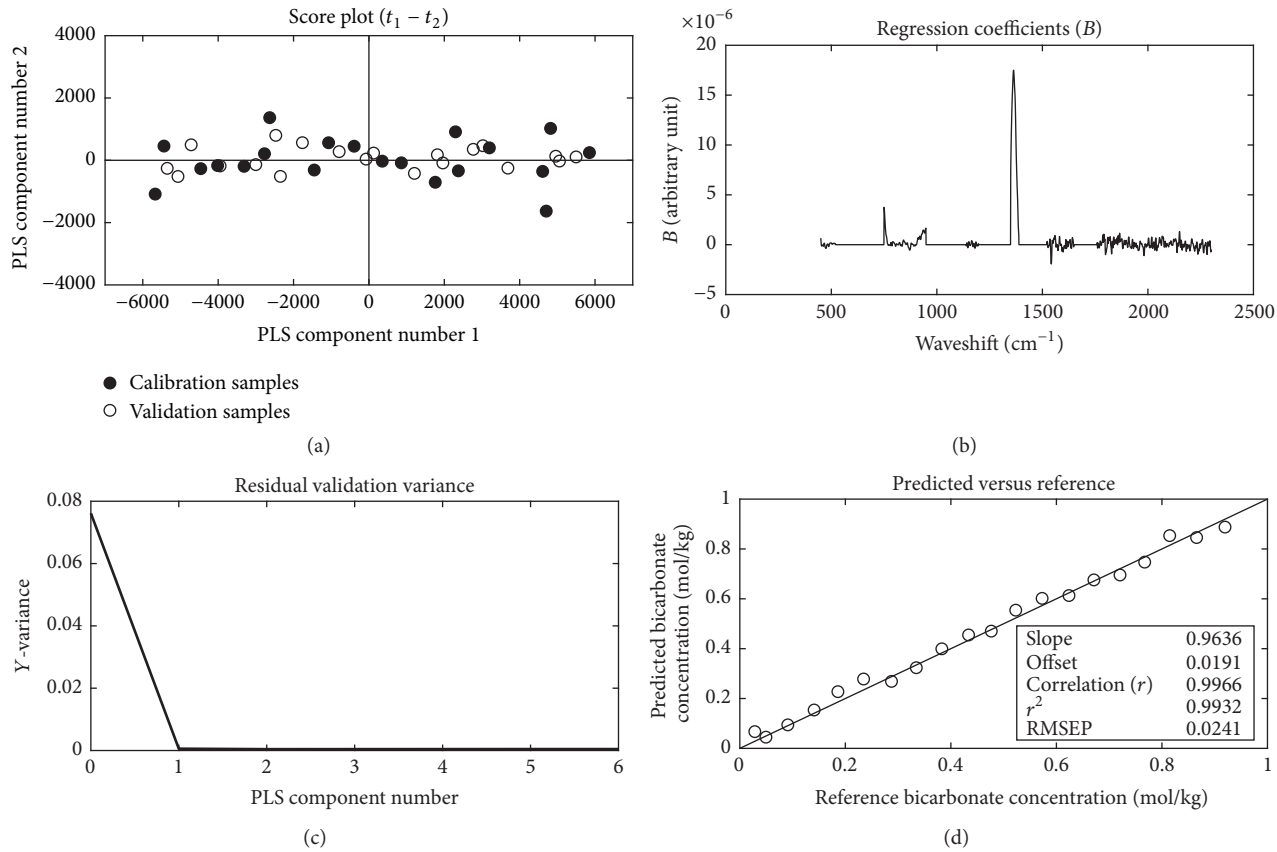

Figure 5: PLS-R model for bicarbonate. (a) Score plot of PLS components 1 versus 2 showing the calibration samples and validation samples. (b) Regression coefficients based on a one-component PLS-R model. (c) The residual validation variance shows that one PLS-component is optimal. (d) Predicted bicarbonate concentrations based on the one-component PLS-R model versus the reference concentrations obtained from the solution preparation stage.

cannot be described by one peak. According to Table 2, vibrational modes assigned to carbonate, bicarbonate, and carbamate fall closer to each other in the finger print area from 1000 to 1420 cm^{-1}. The NH_3-CO_2-H_2O system consists of several equilibrium reactions and the compositions of carbonate, bicarbonate, and carbamate are influenced by the concentrations of each other. It can be seen from the calibration spectrum that there are completely visible, independent nicely shaped peak assigned to each other; however this may be not true when it comes to the real CO_2 loaded ammonia system. Two scenarios of misuse of the multivariate regression in spectroscopic applications have been explained by Esbensen et al. [28]. They are assigning individual peaks for regression which are identified by the preprocessed data or by regression coefficients. The regression coefficients are used to calculate the response value from the X-measurements. The size of the coefficients gives an indication of which variables have an important impact on the response variables. Assigning wavelengths selected during calibration development for regression must be done with caution because more than one wavelengths are associated with the functional group to some degree [28]. Many factors including scatter effect affect the wavelength position and only by using a wavelength region can the robustness of the calibration model be increased.

The score plots shown in Figures 4–6 reveal that the calibration and validation datasets in all three cases span the same score space, which indicates similarity of the datasets. The most important wavelengths are those with regression coefficients that show the largest deviation from zero. The regression coefficients listed in Figure 4 (carbonate), Figure 5 (bicarbonate), and Figure 6 (carbamate) show that the most important wavelength ranges are 1060–1070 cm^{-1}, 1350–1380 cm^{-1}, and 1033–1043 cm^{-1}, respectively. In all three models, only a small contribution is gained from wavelengths outside these ranges. The residual validation variance plot shows that one-component PLS-R is sufficient for all three models. The slope of the regression line is 0.96–1.02 and the r^2 is 0.0.993–0.999, which is close to the optimal value of 1.0. The average prediction errors, that is, RMSEP values, for carbonate, bicarbonate, and carbamate, were 4.3 mmol/kg H_2O, 24.1 mmol/kg H_2O, and 49.9 mmol/kg H_2O, respectively.

3.2. Demonstration of the Method. The proposed speciation method was demonstrated using aqueous solutions of 5 wt% ammonia loaded with CO_2. Since reference concentrations

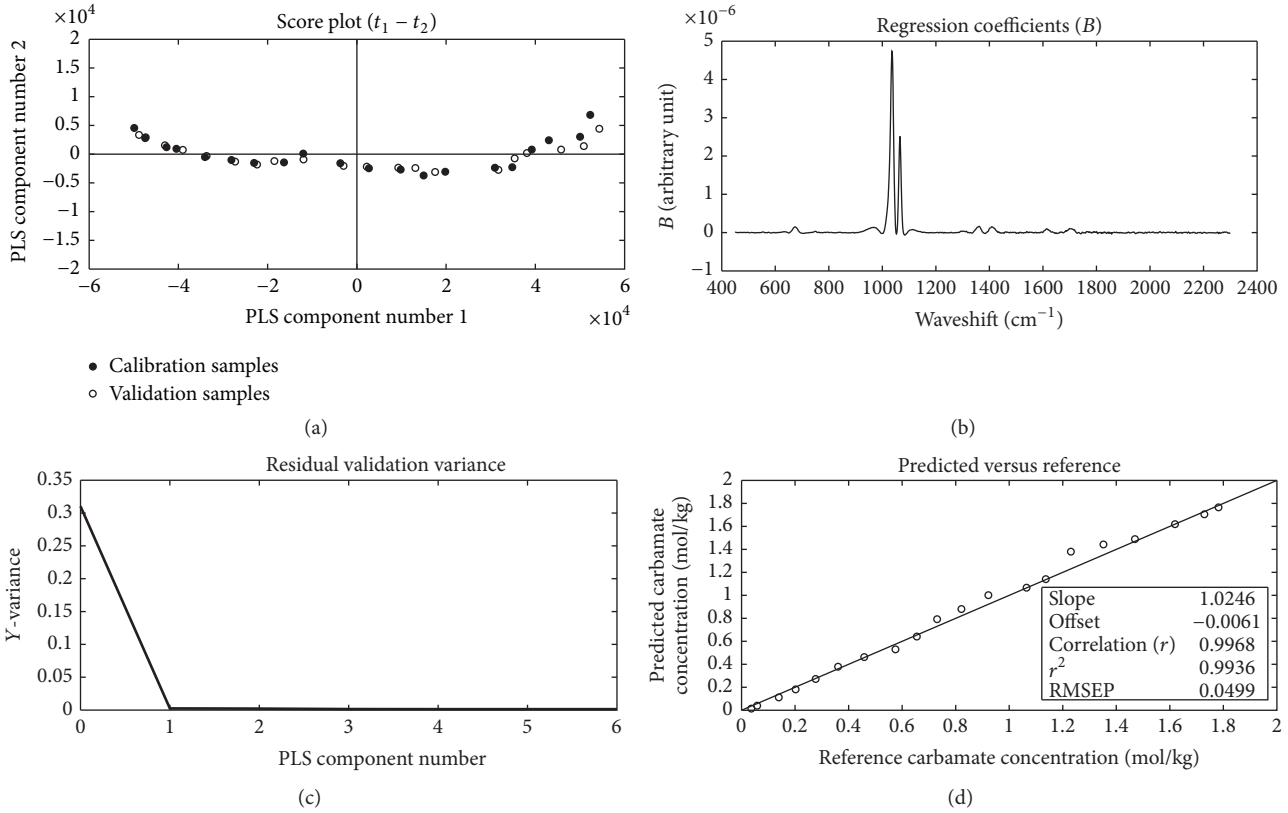

Figure 6: PLS-R model for carbamate. (a) Score plot of PLS components 1 versus 2 showing the calibration samples (filled circles) and validation samples (open circles). (b) Regression coefficients based on a one-component PLS-R model. (c) The residual validation variance shows that one PLS-component is optimal. (d) Predicted carbamate concentrations based on the one-component PLS-R model versus the reference concentrations obtained from the solution preparation stage.

of carbonate, bicarbonate, and carbamate were not available, the prediction performance level of each model was assessed based on the calculated prediction uncertainties, as defined previously [29]. The demonstration dataset was based on 14 solutions with different loadings (mole-ratio CO_2/NH_3) of CO_2, which were measured three times (42 samples in total). The solvent CO_2 loading is one of the primary process parameters in the operation of systems for the chemical absorption of CO_2.

Figure 7 shows the predicted concentrations of the measured species. The average prediction uncertainties for carbonate, bicarbonate, and carbamate were 6.45 mmol/kg H_2O, 34.39 mmol/kg H_2O, and 100.9 mmol/kg H_2O, respectively. Overall, the predictions of the sample solutions with corresponding uncertainties give a satisfactory outcome regarding speciation of all the anions. The last three predictions for carbamate shown in Figure 7(c) reveal greater uncertainties than those noted for the other predictions. This is due to either the precipitation of solids or the presence of a slightly higher concentration of ammonia in this sample. While a precipitate was not visible in this sample, the conditions were close to those for which precipitation is expected. Thus, the influence of precipitation could not be ruled out. In the accompanying report [14], the method presented here is compared to the experimental data of the same samples with the precipitation-titration method, with good agreement. In the present study, the difference observed between the demonstration dataset and the carbamate calibration is that even though all the same species are present, the CO_2 loading differs (see reactions (12) and (13)). In the demonstration dataset, the amounts of ammonia and water are roughly constant, and the amount of CO_2 increases continuously with increasing sample number. In the demonstration dataset, the CO_2 loading is increased from 0 to 0.6. Thus, the present method can relate the CO_2 loading to the liquid carbon distribution through reactions (2)–(5).

3.3. Comparison of the Model with Literature. Three models developed in this study have been used in the study of VLE data of chilled ammonia system [14]. This study shows the model predictability which has been compared with two thermodynamic models of Darde et al. [6] and Que and Chen [24] and experimental work carried out by Wen and Brooker [10], Holmes et al. [8], Zhao et al. [11], and Ahn et al. [30]. The composition analysis performed by Zhao et al. [11] for CO_2-NH_3-H_2O system is based on univariate analysis of Raman measurements. They record results for different initial ammonia concentrations in the

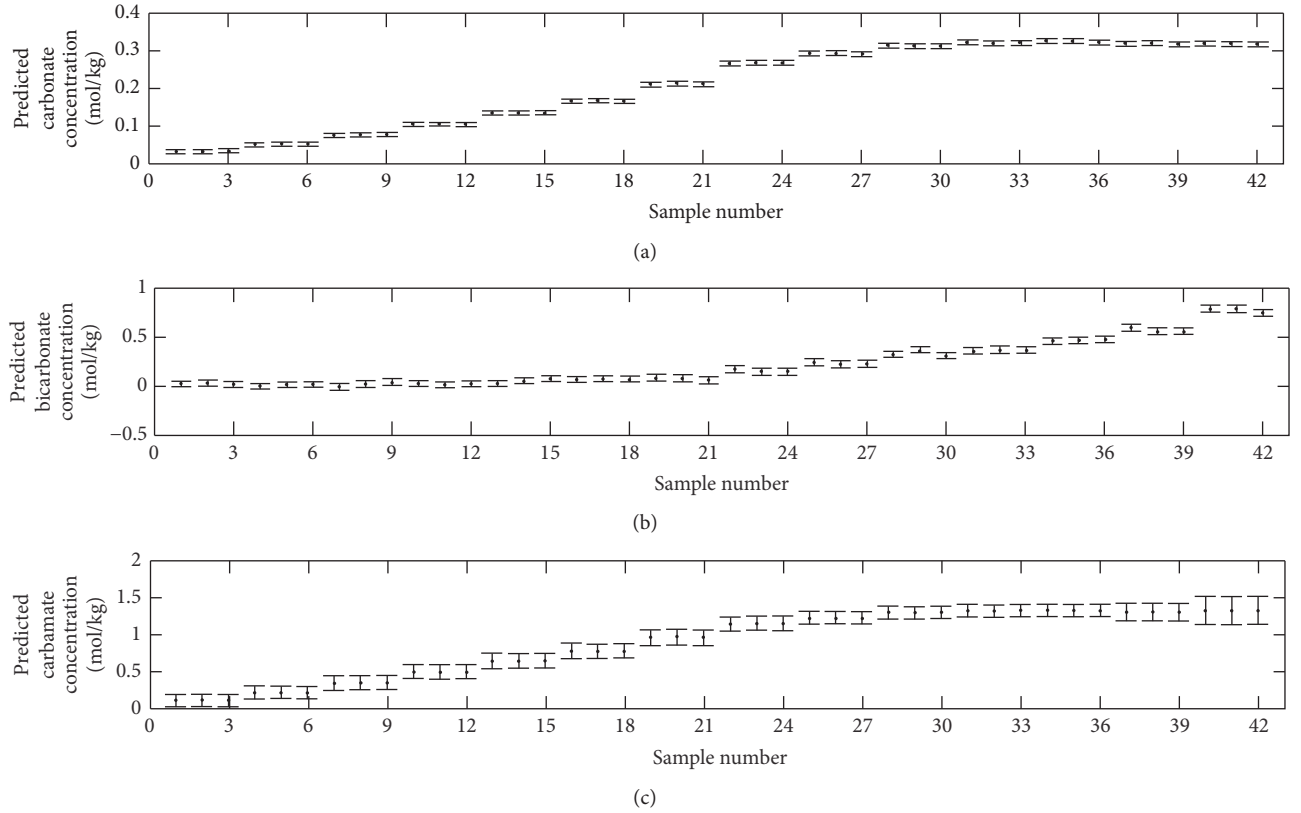

Figure 7: Predicted concentrations [mol/kg] of (a) carbonate; (b) bicarbonate; and (c) carbamate.

range of 0.69 mol/L to 2.10 mol/L and CO_2 concentration range from 0.18 to 0.67 mol/L. The work is related to low concentrations of ammonia. The proposed method in this study is independent of ammonia concentration and is based on three calibration sets each with 20 measurements which were followed by validation using independent data set spanning in the calibration range for each species. Zhao's method includes calculating molar scattering intensity (J) of each carbon species by preparation of series of solutions of sodium carbonate and sodium bicarbonate to calculate J of carbonate and bicarbonate while J of carbamate was calculated by carbon conservation balance. Therefore the molar scattering intensity of carbamate was dependent on those of other 2 components.

4. Conclusion

A method for speciation of the CO_2-NH_3-H_2O system is proposed. The proposed method can be applied without the need for additional analytical calibration methods. Speciation is achieved based on a combination of Raman spectroscopy and multivariate PLS-R modeling, wherein the so-called full spectrum calibration method is applied to extract information from the entire spectrum. The concentrations of carbonate, bicarbonate, and carbamate were predicted with an average prediction error (RMSEP) as being 4.3 mmol/kg H_2O, 24.1 mmol/kg H_2O, and 49.9 mmol/kg H_2O, respectively. For the method demonstration case, which lacked reference concentrations, the prediction uncertainties for carbonate, bicarbonate, and carbamate were 6.45 mmol/kg H_2O, 34.39 mmol/kg H_2O, and 100.9 mmol/kg H_2O, respectively.

Appendix

Concentrations of the Carbonate, Bicarbonate, and Carbamate Species in the Solutions Used for Model Calibration and Validation

See Table 4.

Conflicts of Interest

The authors declare no conflicts of interest regarding the publication of this research paper.

Acknowledgments

The financial support provided by the Norwegian Research Council and the industrial partners in the KMB project (no. 199905/S60) and the Ph.D. scholarship financed by the Ph.D. programme in Process Energy and Automation at University College in Southeast Norway are gratefully acknowledged.

Table 4: Overview of sample solutions reported as mol/kg H_2O.

Sample number	Carbonate [mol/kg H_2O]		Bicarbonate [mol/kg H_2O]		Carbamate [mol/kg H_2O]	
	Calibration	Validation	Calibration	Validation	Calibration	Validation
(1)	0.00000	0.01974	0.00000	0.03441	0.00000	0.07923
(2)	0.03840	0.05585	0.05671	0.05704	0.14939	0.14652
(3)	0.07280	0.09137	0.10508	0.10159	0.29518	0.27757
(4)	0.11073	0.12401	0.15180	0.15504	0.39826	0.40627
(5)	0.14710	0.15777	0.20941	0.20138	0.53542	0.55145
(6)	0.18544	0.19187	0.25647	0.25214	0.67098	0.67585
(7)	0.22126	0.22658	0.30250	0.30090	0.80054	0.80525
(8)	0.25856	0.26310	0.35346	0.35263	0.93483	0.94422
(9)	0.29493	0.29814	0.40131	0.40289	1.08200	1.05871
(10)	0.33113	0.33291	0.46320	0.45270	1.21012	1.21201
(11)	0.36895	0.36560	0.49901	0.49946	1.33941	1.33618
(12)	0.39913	0.40255	0.54737	0.54932	1.47757	1.47498
(13)	0.44205	0.43683	0.59693	0.60006	1.61910	1.60257
(14)	0.47772	0.47227	0.65191	0.65196	1.73472	1.73898
(15)	0.51599	0.50607	0.70127	0.70248	1.87207	1.87232
(16)	0.55162	0.54010	0.74870	0.75143	2.02088	2.01094
(17)	0.59048	0.57554	0.79937	0.79809	2.12369	2.13626
(18)	0.62521	0.61002	0.84721	0.84682	2.27083	2.28208
(19)	0.66210	0.64656	0.90173	0.89758	2.41909	2.41723
(20)	0.69948	0.68035	0.95353	0.94859	2.55658	2.44528

References

[1] S. Solomon, D. Qin, M. Manning et al., "Climate Change 2007: The Physical Science Basis," Contribution of Working Group I to the Fourth Assessment Report of the Intergovernmental Panel on Climate Change, Cambridge University Press, Cambridge, UK, 2007.

[2] IEA, *Technology Roadmap: Carbon Capture and Storage*, International Energy Agency, Paris, France, 2013.

[3] G. T. Rochelle, "amine scrubbing for CO2 capture," *Science*, vol. 325, no. 5948, pp. 1652–1654, 2009.

[4] G. d. Koeijer, Y. O. Enge, C. Thebault, S. Berg, J. Lindland, and S. J. Overå, "European CO2 test centre mongstad–testing, verification and demonstration of post-combustion technologies," *Energy Procedia*, vol. 1, no. 1, pp. 1321–1326, 2009.

[5] O. Lawal, A. Bello, and R. Idem, "The role of methyl diethanolamine (MDEA) in preventing the oxidative degradation of CO2 loaded and concentrated aqueous monoethanolamine (MEA)-MDEA blends during CO2 absorption from flue gases," *Industrial and Engineering Chemistry Research*, vol. 44, no. 6, pp. 1874–1896, 2005.

[6] V. Darde, K. Thomsen, W. J. M. van Well, and E. H. Stenby, "Chilled ammonia process for CO2 capture," *International Journal of Greenhouse Gas Control*, vol. 4, no. 2, pp. 131–136, 2010.

[7] J. T. Yeh, H. W. Pennline, K. P. Resnik, and K. Rygle, *Absorption And Regeneration Studies for CO2 Capture by Aqueous Ammonia*, Pittsburgh, PA, USA, 2004.

[8] P. E. Holmes, M. Naaz, and B. E. Poling, "Ion concentrations in the CO2-NH3-H2O system from 13C NMR spectroscopy," *Industrial and Engineering Chemistry Research*, vol. 37, no. 8, pp. 3281–3287, 1998.

[9] L. Meng, S. Burris, H. Bui, and W.-P. Pan, "Development of an analytical method for distinguishing ammonium bicarbonate from the products of an aqueous ammonia CO2 scrubber," *Analytical Chemistry*, vol. 77, no. 18, pp. 5947–5952, 2005.

[10] N. Wen and M. H. Brooker, "Ammonium carbonate, ammonium bicarbonate, and ammonium carbamate equilibria: a raman study," *Journal of Physical Chemistry®*, vol. 99, no. 1, pp. 359–368, 1995.

[11] Q. Zhao, S. Wang, F. Qin, and C. Chen, "Composition analysis of CO2-NH3-H2O system based on Raman spectra," *Industrial and Engineering Chemistry Research*, vol. 50, no. 9, pp. 5316–5325, 2011.

[12] Y. J. Kim, J. K. You, W. H. Hong, K. B. Yi, C. H. Ko, and J.-N. Kim, "Characteristics of CO2 absorption into aqueous ammonia," *Separation Science and Technology*, vol. 43, no. 4, pp. 766–777, 2008.

[13] P. A. G. L. Samarakoon, N. H. Andersen, C. Perinu, and K.-J. Jens, "Equilibria of MEA, DEA and AMP with bicarbonate and carbamate: a Raman study," *Energy Procedia*, vol. 37, pp. 2002–2010, 2013.

[14] H. Jilvero, K.-J. Jens, F. Normann et al., "Equilibrium measurements of the NH3-CO2-H2O system - measurement and evaluation of vapor-liquid equilibrium data at low temperatures," *Fluid Phase Equilibria*, vol. 385, pp. 237–247, 2015.

[15] K. H. Esbensen, D. Guyot, F. Westad, and L. P. Houmoller, *Multivariate Data Analysis: in Practice*, CAMO Software, Oslo, Norway, 2010.

[16] U. Lichtfers and B. Rumpf, "Infrared spectroscopic studies of the determination of species concentrations in aqueous solutions containing ammonia and carbon dioxide," *Chemie Ingenieur Technik*, vol. 72, pp. 1526–1530, 2000.

[17] U. Lichtfers and B. Rumpf, "An infrared spectroscopic investigation on the species distribution in the system NH3 + CO2 + H2O," *Thermodynamic Properties of Complex Fluid Mixtures*, pp. 92–119, 2004.

[18] J. R. Ferraro, K. Nakamoto, and C. W. Brown, *Introductory Raman Spectroscopy*, Academic Press, San Diego , Calif, USA, 2 edition, 2008.

[19] H. Martens and T. Naes, *Multivariate calibration*, John Wiley & Sons, London, UK, 1989.

[20] K. A. Bakeev, *Process analytical technology: spectroscopic tools and implementation strategies for the chemical and pharmaceutical industries*, John Wiley & Sons, 2010.

[21] K. H. Esbensen and P. Geladi, "Principles of proper validation: use and abuse of re-sampling for validation," *Journal of Chemometrics*, vol. 24, no. 3-4, pp. 168–187, 2010.

[22] A. Seidell, *Solubilities of inorganic and organic compounds; a compilation of quantitative solubility data from the periodical literature*, D. Van Nostrand Company, New York, NY, USA, 2 edition, 1919.

[23] K. S. Pitzer, "Thermodynamics of electrolytes. I. theoretical basis and general equations," *Journal of Physical Chemistry*, vol. 77, no. 2, pp. 268–277, 1973.

[24] H. Que and C.-C. Chen, "Thermodynamic modeling of the NH3-CO2-H2O system with electrolyte NRTL model," *Industrial and Engineering Chemistry Research*, vol. 50, no. 19, pp. 11406–11421, 2011.

[25] E. M. Pawlikowski, J. Newman, and J. M. Prausnitz, "Phase equilibria for aqueous solutions of ammonia and carbon dioxide," *Industrial Engineering Chemistry Research Process Design and Development*, vol. 21, pp. 764–770, 1982.

[26] K. H. Liland, T. Almøy, and B.-H. Mevik, "Optimal choice of baseline correction for multivariate calibration of spectra," *Applied Spectroscopy*, vol. 64, no. 9, pp. 1007–1016, 2010.

[27] P. H. C. Eilers, "A perfect smoother," *Analytical Chemistry*, vol. 75, no. 14, pp. 3631–3636, 2003.

[28] K. Esbensen, P. Geladi, A. Larsen, and P. Williams, "Mythbusters: one can always assign a wavelength/wavelength region specific for one's application," *NIR News*, vol. 26, no. 4, pp. 15–17, 2015.

[29] M. Høy, K. Steen, and H. Martens, "Review of partial least squares regression prediction error in Unscrambler," *Chemometrics and Intelligent Laboratory Systems*, vol. 44, no. 1-2, pp. 123–133, 1998.

[30] C. K. Ahn, H. W. Lee, Y. S. Chang et al., "Characterization of ammonia-based CO2 capture process using ion speciation," *International Journal of Greenhouse Gas Control*, vol. 5, no. 6, pp. 1606–1613, 2011.